GEOPHYSICAL RESEARCH LETTERS, VOL. 26, NO. 16, PAGES 2439-2440, AUGUST 15, 1999

Remote Sensing of Cirrus Cloud Parameters Based on a 0.63 – 3.7 μm Radiance Correlation Technique Applied to AVHRR Data

S. C. Ou and K. N. Liou

Department of Atmospheric Sciences, University of California, Los Angeles, Los Angeles, California

M. D. King and S. C. Tsay

NASA Goddard Space Flight Center, Greenbelt, Maryland

Abstract. Using the data gathered from the Advanced Very High Resolution Radiometer (AVHRR) 0.63 and 3.7 μm channels, an algorithm for the inference of cirrus cloud optical depth and mean effective size has been developed for the first time. This scheme is based on the correlation between the 3.7 μm (total) and 0.63 μm radiances that is constructed from radiative transfer calculations involving ice crystal clouds. Application of the algorithm to AVHRR channels has been performed by using data sets that were collected during the First ISCCP Regional Experiment, Phase II, Cirrus Intensive Field Observation (FIRE-II-IFO; November-December 1991) at Coffeyville, Kansas. For validation, the *in-situ* data collected by the balloon-borne replicator and airborne 2-D probes that were collocated with AVHRR pixels were carefully analyzed for five cases involving single and multiple cirrus cloud layers. We demonstrate that the retrieved cirrus cloud optical depths and mean effective sizes compare reasonably well with those determined from the *in-situ* analyses.

Introduction

Numerous approaches to satellite remote sensing of cirrus cloud optical depth and mean effective size have been developed in the past. These techniques used wavelengths at which absorption by water vapor and other gases is minimal, and at which scattering and absorption by the cloud particles exhibit maximum sensitivity. Ou et al. (1993) developed an IR retrieval scheme using the radiance data from AVHRR 3.7 μm and 10.9 μm channels to infer nighttime cirrus cloud parameters, including cloud temperature, optical depth, and mean effective ice crystal size, based on the theory of radiative transfer and ice microphysics parameterizations. For application of this IR retrieval scheme to daytime conditions, a numerical method to remove the solar component in the 3.7 μm radiance has been developed (Rao et al., 1995). The resulting removal-retrieval program has been applied to AVHRR data collected during both FIRE-I and FIRE-II IFO with validations of the retrieved cirrus cloud parameters based on the collocated *in-situ* ice crystal size distributions collected from 2-D probes and ground-based lidar return imageries (Ou et al., 1995, 1996).

Paper number 1999GL900554.
0094-8276/99/1999GL900554$05.00

Nakajima and King (1990) and King et al. (1997) have developed a solar (daytime) retrieval technique for the determination of water cloud optical depths and effective droplet radii based on the correlation of bidirectional reflectances of visible and near-IR wavelengths. The underlying principle for this technique is based on the fact that the reflection function of clouds at a non-absorbing wavelength in the visible spectral region is primarily a function of the cloud optical depth, whereas the reflection function at a water absorbing wavelength in the near-IR spectral region (e.g. 1.6 and 2.13 μm wavelengths) is primarily a function of the cloud particle size.

In this paper, we first demonstrate that the two-channel correlation technique involving 0.68/1.6 μm and 0.68/2.13 μm pairs can also be applied to the retrieval of the optical depth and mean ice crystal size of cirrus clouds. Neither 1.6 μm nor 2.13 μm is available on the operational satellites at present. However, we will illustrate that the aforementioned correlation approach which is applied to the AVHRR 0.63 μm and 3.7 μm (total radiance) channels can be utilized to infer cirrus cloud optical depth and ice crystal mean size. We will show results of the application of this technique to the AVHRR data collected during FIRE-II-IFO, as well as validation and practical significance.

Two-channel Correlation Techniques

The basic principle of the two-channel correlation technique for the determination of cirrus cloud optical depth and ice crystal size is demonstrated in Fig. 1. Radiative transfer calculations using the MAS (MODIS Airborne Simulator; King et al., 1996) channels of 0.681, 1.617, and 2.139 μm were performed for the six ice crystal size distributions described in Rao et al. (1995), and for two water droplet size distributions with mean effective radii of 4 and 8 μm. The results are displayed in two-dimensional reflectance diagrams in terms of 0.681-1.617 μm and 0.681-2.139 μm for optical depths ranging from 0.5 to 64. For both cirrus and water clouds, the 0.681 μm reflectance mainly depends on the optical depth, whereas the 1.617 and 2.139 μm reflectances are primarily functions of the mean effective particle size. A clear distinction is seen between the correlations for water clouds (mean effective radius < 8 μm) and for cirrus clouds (mean effective size > 20 μm). It is possible that the correlations for larger water droplet mean effective radius and for smaller ice crystal mean effective size may overlap.

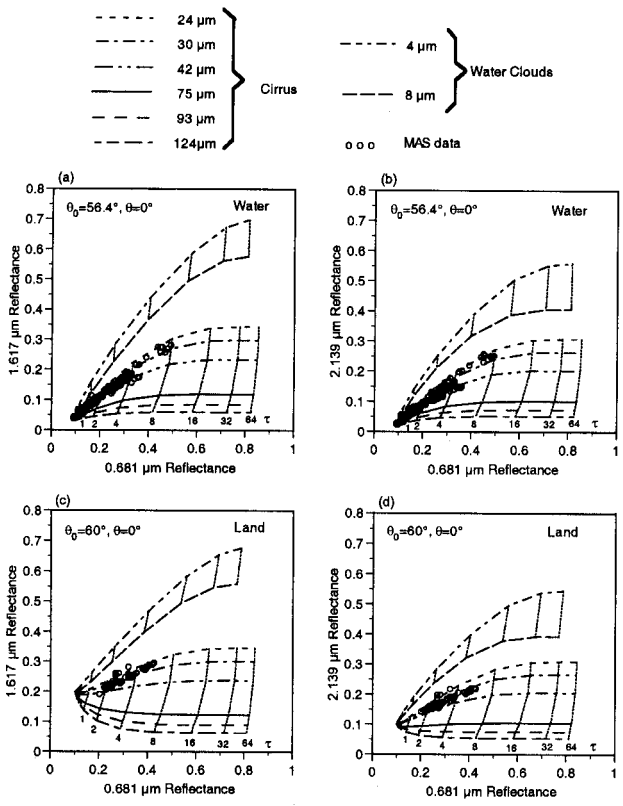

Figure 1. Display of the MAS data taken from FIRE-II-IFO over both land and water surfaces. The plane-parallel radiative transfer calculations were performed for the six ice crystal size distributions with mean effective sizes ranging from 23.9 to 123.6 μm, and for two water clouds with mean effective radii of 4 and 8 μm. The optical depth ranges from 0.5 to 64. Overlapped with the curves are the MAS data obtained from FIRE-II-IFO on 5 December 1991. The data for the water surface was collected at 1636 UTC over the northern Gulf of Mexico, and for the land surface, the data was collected at 1923 UTC over eastern Oklahoma.

However, based on the statistics of aircraft observations compiled by Liou (1992), the mean droplet radius for various water clouds is within the range 3.5 – 5.0 μm (Table 4.2), and the spectra of ice crystal size distribution are generally between 20 and 2000 μm (Table 4.3). Therefore, it is expected that the probability of occurrence of overlap of the correlations for water and ice clouds is very small. Even if the water droplets and ice crystals have about the same sizes, they can be distinguished by their differences in the cloud phase determination separate from the retrieval (Ou et al., 1996) and cloud temperature (Rao et al., 1995).

Also shown are the MAS data obtained from FIRE-II-IFO on 5 December 1991. The top and bottom diagrams correspond to the cases over water and land surfaces, respectively. The case over water was taken at 1636 UTC, 5 December 1991, when the ER-2 was flying over the northern part of the Gulf of Mexico near the southern coastal region of Louisiana. The case over land was taken at 1923 UTC on the same date, when the ER-2 was flying over eastern Oklahoma. In the calculations, the effective surface albedos used were determined from the MAS reflectances over clear pixels that were identified from a scheme similar to the one developed by Ou et al. (1996). The data points indicate that the detected cirrus clouds appear to contain small ice particles with optical depths less than about 6. Larger optical depths indicate the possibility of cirrus overlying low clouds. For each data point, an optical depth and a mean effective ice crystal size can be determined. However, collocated and coincident *in-situ* ice microphysics data were not available for validation.

The 3.7 μm radiance includes both the solar reflection and the thermal emission components. However, the present retrieval technique does not require the removal of either component, and thus is more straightforward and simplified than algorithms involving the same two channels but requiring the adjustment of the 3.7 μm radiance cited in the Introduction. In the computations, we use 10 optical depths ranging from 0.125 to 64. We also use the six ice crystal size distributions described in Rao et al. (1995). The adding-doubling radiative transfer program (Takano and Liou 1989) has been employed to compute the 0.63 μm reflectance and the 3.7 μm total radiance.

Figure 2 shows an example of the relationship between the 0.63 μm reflectance and the 3.7 μm radiance for the six ice crystal size distributions. The prescribed viewing geometry is based on the orbital information for a daytime NOAA-11 overpass near southeast Kansas at 2108 UTC, 5 December 1991. The nearly vertical dotted lines are curves of constant optical depth, where the value of the associated optical depth is given near the bottom of each curve. The dashed and solid lines are curves of constant mean effective ice crystal size, where the value of the associated mean effective ice crystal size is given in the legend. None of the constant optical depth and constant mean effective size curves overlaps, indicating that any point within the correlation mesh corresponds to a unique combination of optical depth and mean effective size. As in Fig. 1, the 0.63 μm reflectance mainly depends on the optical depth. It is noted that reflectances/radiances of both channels converge to their respective clear values for thin (small optical depth) cirrus. The 3.7 μm radiances of constant mean effective size reach asymptotic values for optical depths

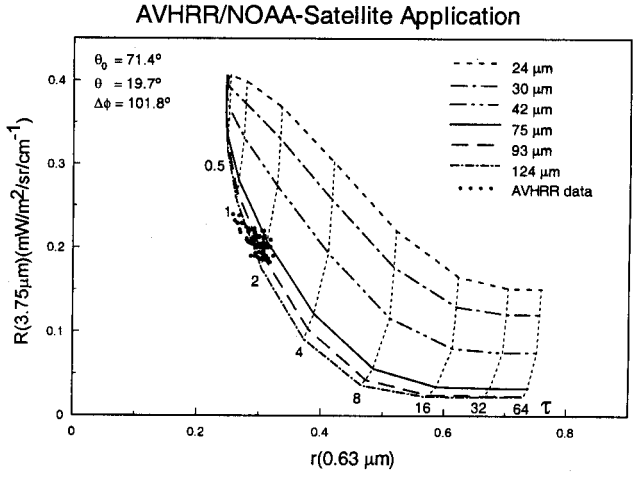

Figure 2. An example of correlations between 0.63 μm reflectance and 3.7 μm radiance based on radiative transfer parameterizations. Dotted lines are curves of the constant optical depth. Legends denote curves of the constant mean ice crystal effective size. Also shown are the AVHRR data collected on 5 December 1991 over a small area collocated with the replicator sounding for ice particles.

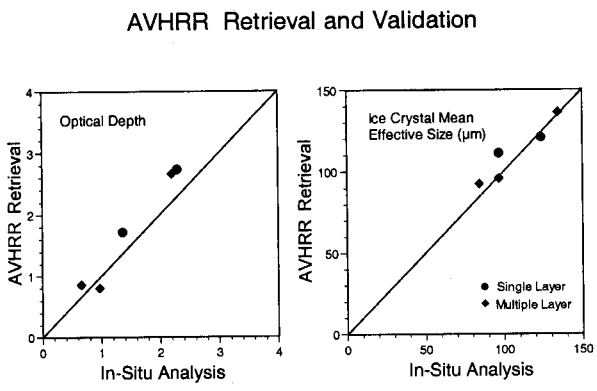

Figure 3. Comparison of the retrieval results inferred from the 0.63-3.7 μm correlation technique with those determined from *in-situ* analyses for five carefully selected cirrus cases. The diagonal lines represent equality between the retrieved and *in-situ* analyzed values.

larger than 16 due to saturated absorption by clouds with larger optical depths. Moreover, this asymptotic value decreases with increasing mean effective size, because with increasing mean effective size, the single-scattering albedo decreases, while the asymmetric factor increases. Finally, the asymptotic dependence on the mean effective size becomes weaker for sizes larger than 100 μm. Uncertainties in this type of two-channel correlation caused by variations of cloud and surface properties have been discussed in Nakajima and King (1990) and King et al. (1997).

The preceding analyses have the following implications. First, the accurate retrieval of thin cirrus cloud parameters depends on both 0.63 μm clear reflectance and 3.7 μm clear radiance values. This dependence becomes less significant for optically thicker cirrus clouds. Thus, it is important to specify both 0.63 μm clear reflectance and 3.7 μm clear radiance values accurately to achieve reliable accuracy in the retrieval of thin cirrus cloud parameters. Estimates of the 0.63 μm clear reflectance and 3.7 μm clear radiance are obtained based on statistics of satellite measured radiances for all detected clear pixels (Ou et al. 1996; Rao et al. 1995). These estimates of clear radiative parameters contain the effects of the surface and atmospheric contributions below the cloud, including aerosols. We can improve the accuracy from the auxiliary information about surface reflectivity, emissivity, and temperature, as well as the aerosol profile. Further, due to the asymptotic behavior of the 3.7 μm radiance for optically thick cirrus, it is reasonable to make an initial estimate of the mean effective size directly from the 3.7 μm radiance. Likewise, due to a strong dependence of the 0.63 μm reflectance on optical depth, it is also physically appropriate to make a first guess of the optical depth based solely on the 0.63 μm reflectance.

Overlapped with the curves in Fig. 2 are the NOAA-11 AVHRR 0.63 μm reflectance and 3.7 μm radiance data over a 0.05° x 0.2° area near the balloon launch site. The location of the area was chosen so that it is collocated and coincident with balloon-borne replicator sounding measurements. Most of the data are located between the optical depth curves of 1 and 2, and between the mean effective ice crystal size curves of 75 and 124 μm. A few points fall outside the correlation mesh, indicating that the mean effective ice crystal sizes associated with these points could be larger than 124 μm.

Our retrieval algorithm is based on comparison of the measured and pre-computed 0.63 μm reflectance and 3.7 μm radiance values. For this purpose, an estimate of the mean cloud temperature is required. We define the square sum of differences between the measured ($R_{4i,mea}$) and computed ($R_{4i,com}$) 10.9 μm radiances:

$$\chi^2 = \sum_i (R_{4i,mea} - R_{4i,com})^2, \tag{1}$$

where i is the pixel index. The parameter $R_{4i,com}$ can be evaluated based on the radiative transfer parameterization developed by Ou et al. (1993, 1995, 1998) as follows:

$$R_{4i,com} = (1-\varepsilon_{4i})R_{a4} + \varepsilon_{4i}B_4(T_c), \tag{2}$$

where R_{a4} is the mean clear radiance, $B_4(T_c)$ is the 10.9 μm Planck function at the mean cloud temperature, T_c, and ε_{4i} is the 10.9 μm cloud emissivity. Following the approach developed by Liou et al. (1990), ε_{4i} can be parameterized in terms of the optical depth, τ_i, in the form

$$\varepsilon_{4i} = 1 - \exp(-k_4\tau_i), \tag{3}$$

where k_4 is the effective extinction coefficient, which accounts for multiple scattering within cirrus clouds and the difference between visible and IR extinction coefficients. By combining Eqs. (1) - (3), and by minimizing χ^2, we obtain the mean cloud temperature as follows:

$$B_4(T_c) = \frac{\sum_i [\varepsilon_{4i}R_{4i,mea} - \varepsilon_{4i}(1-\varepsilon_{4i})R_{a4}]}{\sum_i \varepsilon_{4i}^2}. \tag{4}$$

Using a prescribed mean effective size, a cloud optical depth is determined by matching the computed and measured 0.63 μm reflectance using a straightforward linear interpolation scheme. It follows that T_c can be computed from Eq. (4).

Based on this mean cloud temperature, we establish a correlation between the 0.63 μm reflectance and the 3.7 μm radiance as described above. Subsequently, we search for a combination of optical depth and mean effective size by defining a residual term :

$$\begin{aligned} E^2 = &[\ln|r_{1i,mea} - r_{1i,com}(\tau_i, D_{ei})|]^2 \\ &+ [\ln|R_{3i,mea} - R_{3i,com}(\tau_i, D_{ei})|]^2, \end{aligned} \tag{5}$$

where $r_{1i,mea}$ and $r_{1i,com}$ are the measured and computed 0.63 μm reflectances, and $R_{3i,mea}$ and $R_{3i,com}$ are the measured and computed 3.7 μm radiances, respectively. Finally, we use a systematic search method coupled with a linear interpolation scheme to find the solutions for optical depth and mean effective size by minimizing E^2. The above computational steps are repeated until the cloud temperature, optical depth and mean effective size all converge.

Application to FIRE-II-IFO Measurements

The preceding cirrus cloud retrieval scheme is applied to the AVHRR-HRPT (~1km x 1km resolution) data obtained during FIRE-II-IFO. We focus on five cases: 5 December, and 26, 28 (2), and 29 November 1991. For these cases, both sounding observations and lidar backscattering measurements indicated the presence of cirrus clouds. Moreover, the cases of 28 and 29 November contain cirrus clouds overlying overcast or broken lower stratus clouds around the observation site. For validation purposes, we have also analyzed the balloon-

borne replicator data and the airborne 2-D probe data, the latter obtained from the NCAR King Air turboprop. During FIRE-II-IFO, balloon-borne formvar ice crystal replicators were launched to measure the "vertical profiles" of cirrus microphysical properties, with emphasis on the detection of small ice particles. Replicator launches on 5 December and 26 and 29 November were timed to coincide with NOAA satellite overpasses. The aircraft flight on 28 November was nearly concurrent with the NOAA-11 overpass. The replicator launched on 28 November was between the NOAA-11 and -12 overpasses. We have followed the analytical models developed by Ou et. al. (1995) to compute the optical depth and ice crystal mean effective size from both the replicator and 2-D probe data.

Figure 3 shows the comparison of the five cases of retrieval results from the 0.63-3.7 μm correlation technique with those from the *in-situ* analyses. The cases of single- and multi-layer cirrus clouds are represented by solid circles and diamonds, respectively. The diagonal lines represent equality between the retrieved and *in-situ* analyzed values. Above (below) these lines, the retrieved value is larger (smaller) than the *in-situ* value. Most of the retrieved optical depths are slightly larger than the *in-situ* values by an average of about 15%. This difference could be partly attributed to the uncertainty in the specification of the 0.63 μm clear and low cloud reflectances for single- and multi-layer cirrus cloud conditions, respectively, as well as to the assumption of a mean cloud temperature within the retrieval domain. The retrieved mean effective ice crystal sizes, on the other hand, are close to the *in-situ* values with an average difference of about 3.6 μm. This excellent agreement is probably a result of the lesser sensitivity of 3.7 μm radiance to the reflection and emission properties of surface and low clouds.

Concluding Remarks

An algorithm for the retrieval of cirrus cloud optical depth and mean effective size using a 0.63 – 3.7 μm channel radiance correlation technique has been developed. The 3.7 μm radiance includes both solar reflection and thermal emission components, and the technique does not require the removal of either component. The algorithm is based on the fundamental theories of light scattering by non-spherical ice crystals and radiative transfer in cirrus clouds. The reflectance correlation diagrams are constructed using representative ice crystal size and shape distributions and a line-by-line equivalent adding-doubling radiative transfer model. To validate the algorithm, we have selected five cases of the FIRE-II data over the southeastern Kansas area during the period from mid-November to early December, 1991. These cases included both single and multi-layer cirrus clouds. The retrieved cirrus cloud parameters are shown to be comparable to those derived from collocated and coincident balloon-borne replicator sounding and airborne cloud probe data. The present 0.63 and 3.7 μm radiance correlation scheme can be directly applied to the operational AVHRR/NOAA channels to produce the optical depth and ice crystal size of cirrus clouds over the globe.

Acknowledgements. Research supported by NASA Grants NAG5-6160, NAG5-7738, and NAG1-1966, managed in part by Dr. Robert Curran of the Radiation Branch, NASA Headquarter.

References

King, M. D., W. P. Menzel, P. S. Grant, J. S. Myers, G. T. Arnold, S. E. Platnick, L. E. Gumley, S. C. Tsay, C. C. Moeller, M. Fitzgerald, K. S. Brown, and F. G. Osterwisch, Airborne scanning spectrometer for remote sensing of cloud, aerosol, water vapor and surface properties, *J. Atmos. Oceanic Technology, 13*, 777-794, 1996.

King, M. D., S.-C. Tsay, S. E. Platnick, M. Wang, and K. N. Liou, Cloud retrieval algorithms for MODIS: Optical thickness, effective particle radius, and thermodynamic phase, *MODIS Algorithm Theoretical Basis Document, No. ATBD-MOD-05*, 1997[at http://eospso.gsfc.nasa.gov/atbd/modistables.html].

Liou, K. N., *Radiation and Cloud Processes in the Atmosphere*, 487pp., Oxford Press, NY, 1992.

Liou, K. N., S. C. Ou, Y. Takano, F. P. J. Valero, and T. P. Ackerman, Remote sounding of the tropical cirrus cloud temperature and optical depth using 6.5 and 10.5 μm radiometers during STEP, *J. Appl. Meteor., 29*, 716-726, 1990.

Nakajima, T., and M. D. King, Determination of the optical thickness and effective particle radius of clouds from reflected solar radiation measurements, Part I. Theory, *J. Atmos. Sci., 47*, 1878-1893, 1990.

Ou, S. C., K. N. Liou, W. M. Gooch, and Y. Takano, Remote sensing of cirrus clouds parameters using AVHRR 3.7 and 10.9 μm channels, *Appl. Opt., 32*, 2171-2180, 1993.

Ou, S. C., K. N. Liou, and Coauthors, Remote sounding of cirrus cloud optical depths and ice crystal sizes from AVHRR data: Verification using FIRE-II-IFO measurements. *J. Atmos. Sci., 52*, 4143-4158, 1995.

Ou, S. C., K. N. Liou, and B. A. Baum, Detection of multilayer cirrus cloud systems using AVHRR data: Verification based on FIRE-II-IFO composite measurements, *J. Appl. Meteor., 35*, 178-191, 1996.

Ou, S. C., K. N. Liou, and T. R. Caudill, Remote sounding of multilayer cirrus cloud systems using AVHRR Data collected during FIRE-II-IFO, *J. Appl. Meteor., 37*, 241-254, 1998.

Rao, N. X., S. C. Ou, and K. N. Liou, Removal of solar component in the AVHRR 3.7 μm radiances for the retrieval of cirrus cloud parameters. *J. Appl. Meteor., 34*, 482-499, 1995.

Takano, Y., and K. N. Liou, Solar radiative transfer in cirrus clouds. Parts I & II. *J. Atmos. Sci., 46*, 3-36, 1989.

S. C. Ou, K. N. Liou, University of California, Los Angeles, Department of Atmospheric Science, Los Angeles, CA 90095-1565.

M. D. King, S. C. Tsay, NASA Goddard Space Flight Center, Code 900, Greenbelt, MD 20771.

(Received: May 3, 1999; revised: June 17, 1999; accepted: June 22, 1999)